JOURNAL OF SOLID STATE CHEMISTRY 120, 74–79 (1995)

Crystal Chemistry of Noncentrosymmetric Alkali-Metal Nb and Ta Oxide Pyroborates

Annapoorna Akella and Douglas A. Keszler[1]

Department of Chemistry and Center for Advanced Materials Research, Oregon State University, Gilbert Hall 153, Corvallis, Oregon 97331-4003

Received November 21, 1994; accepted June 28, 1995

The compounds $CsNbOB_2O_5$ and $CsTaOB_2O_5$ have been synthesized and structurally characterized by single-crystal X-ray diffraction methods. Each crystallizes with two formula units in the orthorhombic system and space group $Pmn2_1$. Cell parameters for the Nb compond are $a = 7.527(2)$, $b = 3.988(1)$, $c = 9.717(2)$ Å, and $V = 291.7(2)$ Å^3; cell parameters for the Ta compound are $a = 7.5479(9)$, $b = 3.9064(4)$, $c = 9.7713(9)$ Å, and $V = 288.11(9)$ Å^3. The structures of these materials are compared to those of $RbNbOB_2O_5$ and $KNbOB_2O_5$, and results are correlated to the linear and nonlinear optical properties of the crystals. X-ray data on the solid-solution series $Rb_{1-x}K_xNbOB_2O_5$ and $Rb_{1-x}Cs_xNbOB_2O_5$ are also presented. © 1995 Academic Press, Inc.

INTRODUCTION

Because of their structural characteristics, selected compounds of the type $AMOB_2O_5$ (A = K, Rb, Tl; M = Nb, Ta) have recently been studied for their potential as new nonlinear optical materials. The first member of this family, $TlNbOB_2O_5$, was reported by Gasperin in 1974 (1). The derivatives $RbNbOB_2O_5$, $TlTaOB_2O_5$, and $RbTaOB_2O_5$ were described later (2–4), and recently the K derivative, $KNbOB_2O_5$, has been synthesized (5).

Optical studies on single crystals of $KNbOB_2O_5$ and $RbNbOB_2O_5$ have revealed that their second-order nonlinear susceptibilities are approximately five times larger than that of KDP (potassium dihydrogen phosphate). In addition, the birefringence of the Rb derivative is sufficient to phase match 1-μm light. The commercial development of the Rb compound, however, has been thwarted by its tendency to delaminate during fabrication processes (6). During the course of the development of this family of materials, we independently initiated an investigation of its derivative chemistry.

We report here the existence and structures of the two new Cs analogs $CsNbOB_2O_5$ and $CsTaOB_2O_5$ and solid-solution behavior in the series $Cs_{1-x}Rb_xNbOB_2O_5$ and $Rb_{1-x}K_xNbOB_2O_5$. From these results, we establish direct relationships between the structural features of the $AMOB_2O_5$ family and the observed optical properties.

EXPERIMENTAL

Powders of the Nb and Ta oxide borates containing Cs were synthesized by employing high-temperature solid-state methods. Stoichiometric quantities of the starting reagents, alkali-metal precursors (AESAR, nitrates, or carbonates ≥99.9%), and Ta or Nb pentoxide (AESAR, ≥99.9%) were mixed with a 5 mole% excess of B_2O_3, ground under hexane, placed in Pt crucibles, and heated at 923 K for 2 hr to decompose the reagents and initiate the reactions. The samples were cooled, reground, and heated for 12 hr at 1073 K. Compounds in the solid–solution series $Rb_{1-x}K_xNbOB_2O_5$ and $Rb_{1-x}Cs_xNbOB_2O_5$ ($0 \le x \le 1$) were also prepared according to the above prescription. Powder diffraction data were collected on an automated Philips diffractometer with Cu$K\alpha$ radiation; peak positions were corrected by using NIST Si Standard 640b. The *hkl* assignment of each reflection was determined by comparison to indexed patterns of the material $RbNbOB_2O_5$. Unit-cell parameters a, b, and c were refined by least-squares analysis (POLSQ) with fourteen peaks in the range $22° \le 2\theta \le 60°$. The results from the solid solution indicated that the end member $CsNbOB_2O_5$ does exist, adopting a structure similar to that of $RbNbOB_2O_5$.

Single crystals of $CsNbOB_2O_5$ were grown with a flux of $CsCl:B_2O_3$ (1:1) and a compound to flux ratio of 2:1. The melt was cooled from 1273 to 873 K at 8 K/hr and then to room temperature at 50 K/hr. The crystals were isolated by dissolving the flux in hot water. Single crystals of $CsTaOB_2O_5$ were grown from a flux of $Cs_2SO_4:CsCl$ (1:1) with a compound to flux ratio of 2:1 and the same cooling schedule as described above. Crystals of $CsNbOB_2O_5$ and $CsTaOB_2O_5$ with edge lengths near 0.1 mm were selected and mounted on glass fibers with epoxy for structure determination. All measurements were made on a Rigaku AFC6R single-crystal diffractometer

[1] To whom correspondence should be addressed.

0022-4596/95 $12.00

with graphite-monochromated Mo$K\alpha$ radiation. Cell constants and the orientation matrix for data collection were obtained from least-squares refinements with 20 automatically-centered reflections in the range $30° \leq 2\theta \leq 36°$. The cell constants correspond to the orthorhombic crystal system, and Laue symmetry *mmm* was determined on the diffractometer. Extensive, prolonged data collections were conducted on the diffractometer to identify possible supercell reflections; none were found. For each crystal, intensity data were collected over the range of indices $0 \leq h \leq 12$, $0 \leq k$ 16, and $-6 \leq l \leq 6$ by using the ω scan technique to a maximum 2θ value of 75°. From 1572 measured reflections for $CsNbOB_2O_5$, a total of 869 were observed $[F_o^2 > 3\sigma(F^2)]$, and from 1570 reflections for $CsTaOB_2O_5$ a total of 927 data were observed. The intensities of three representative reflections measured after every block of 200 data varied by an average of 0.2% for $CsNbOB_2O_5$ and 0.3% for $CsTaOB_2O_5$ during the collection.

The structures were solved by using the TEXSAN crystallographic software package (7). Each crystal was found to form in the noncentrosymmetric space group $Pmn2_1$. The positions of the Cs and Nb(Ta) atoms were derived from the direct methods program SHELXS (8), while the remaining atoms O and B were located from difference electron density maps. After full-matrix, least-squares refinements of the models with isotropic displacement coefficients on each atom, absorption corrections were applied with the program DIFABS (9), (transmission factors = 0.92–1.12 for $CsNbOB_2O_5$ and 0.86–1.26 for $CsTaOB_2O_5$). The data were averaged (R_{int} = 0.032 for $CsNbOB_2O_5$ and 0.043 for $CsTaOB_2O_5$), and the models were then refined with anisotropic displacement coefficients on each atom except for atom O3 in $CsTaOB_2O_5$. Final least-squares refinements resulted in the residuals R = 0.022 and R_w = 0.028 for $CsNbOB_2O_5$ and R = 0.054 and R_w = 0.066 for $CsTaOB_2O_5$. Neutral atom scattering factors were used in each refinement (10). The final refinement cycle converged in each case with Δ/σ = 0.01, and the maximum peaks in the final electron density maps correspond to 2.37% and 1.97% of a Nb and Ta atom, respectively. Crystal data are outlined in Table 1, and atomic positional and displacement parameters are listed in Table 2. The data in these tables are derived from refinements producing residuals that are lower than those for the corresponding enantiomers.

TABLE 1
Crystal Data and Experimental Conditions for $CsMOB_2O_5$

	M = Nb	M = Ta
Diffractometer	Rigaku AFC6R	
Radiation	Graphite monochromated Mo$K\alpha$ (λ = 0.70629 Å)	
Formula wt. (u)	400.92	431.47
Unit cell	Orthorhombic	
a (Å)	7.527(2)	7.5479(9)
b (Å)	3.988(1)	3.9064(4)
c (Å)	9.717(2)	9.7713(9)
V(Å^3)	291.7(2)	288.11(9)
Space group	$Pmn2_1$ (No. 31)	
D_{calc} (g cm^{-3})	3.910	4.973
F(000)	308	372
Z	2	
Linear abs. coeff. (cm^{-1})	80.471	249.99
No. unique data with $F_o^2 > 3\sigma(F_o^2)$	869	927
$R(F_o)$[a]	0.023	0.054
$R_w(F_o)$	0.029	0.066

[a] Function minimized:

$$\sum_i w_i(|F_o|_i - |F_c|_i)^2; w = \frac{1}{\sigma^2(F_o)}$$

RESULTS AND DISCUSSION

The compounds $CsNbOB_2O_5$ and $CsTaOB_2O_5$ crystallize in the orthorhombic noncentrosymmetric space group $Pmn2_1$. They are isotypic to the structure of $RbNbOB_2O_5$, but they adopt a subcell configuration. A labeled diagram representing the contents of a unit cell is given in Fig. 1.

A three-dimensional framework (Fig. 2) results from the condensation of $Nb(Ta)B_2O_9$ units (Fig. 3), where each unit may be described as the conjunction of a Nb(Ta)-centered distorted O octahedron and a B_2O_5 (pyroborate) group. By sharing vertices, adjacent units fuse to give layers of B_2O_5 groups that are slightly tilted out of the *ac* plane. The O3 atoms, resting above and below the primary plane of the ring system, are shared between adjacent layers only by the Nb(Ta) atoms to give nearly linear $\cdots$ O–Nb(Ta)–

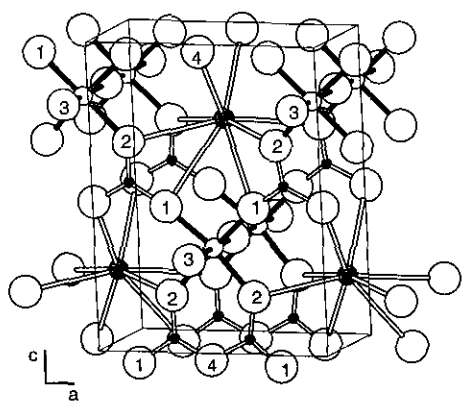

FIG. 1. Labeled drawing of the structure of $CsNbOB_2O_5$ as viewed approximately along the b axis. The large open circles represent O atoms, the medium shaded atoms represent Cs atoms, and the small filled circles represent B atoms, here, and in ensuing figures.

TABLE 2
Positional and Equivalent Displacement Parameters (B_{eq}) for $CsMOB_2O_5$

	M = Nb				M = Ta			
	x	y	z	B_{eq}	x	y	z	B_{eq}
Cs	0	0.4270(1)	0.2262	1.55(2)	0	0.4731	0.3865(2)	1.63(5)
M	0	0.1148(1)	0.8349	0.52(2)	0	−0.0790	0.7753	0.47(2)
O1	0.1902(6)	0.063(1)	0.9585(5)	1.6(2)	−0.191(3)	−0.046(5)	0.635(2)	2.3(7)
O2	0.1782(6)	0.054(1)	0.6830(4)	1.1(1)	0.177(2)	−0.039(5)	0.923(2)	1.1(4)
O3	0	0.560(1)	0.8358(9)	1.8(2)	0	−0.5658	0.789(3)	2.2(4)
O4	0	0.965(2)	0.4809(6)	1.3(2)	0	0.0176	0.128(2)	1.8(7)
B	0.6633(8)	0.009(1)	0.04779(6)	1.0(2)	0.335(3)	−0.021(5)	0.561(2)	1.3(5)

Note. $B_{eq} = \frac{8\pi^2}{3} \sum_i \sum_j U_{ij} a_i^* a_j^* a_i \cdot a_j$.

O–Nb(Ta)–O ··· chains that extend along the b axis.The structure is completed by placement of a Cs atom in an eight-coordinate site within the framework.

Interatomic distances and angles are listed in Table 3. Average Cs–O distances, 3.20 ± 0.08 and 3.18 ± 0.06 Å, and B–O distances, 1.37 ± 0.03 and 1.36 ± 0.05 Å, for the Nb and Ta derivatives, respectively, are consistent with the sum of crystal radii (11). The longer B–O4 distances (cf. Table 3) are also consistent with the trend of lengthened B–O interactions about the central O atom of a pyroborate group (12). As a mirror plane bisects the principal plane of the B_2O_5 group (through the central O atom), the group itself is planar. It is tilted from the ac plane by 2.0° in the case of the Nb analog and by 2.5° in the Ta analog.

A pyramidal distortion of the Nb-centered octahedron is evident, in part, from the angle O1–Nb–O2 = 165.9(2)°; the Nb atom rests 0.22 Å out of the equatorial plane defined by the O1 and O2 atoms. The distortion is less severe in the Ta analog where the angle O1–Ta–O2 = 170.9(6)°, and the Ta atom is displaced from the equatorial plane by only 0.14 Å. The octahedra are further distorted along the axial direction by the occurrence of one short and one long Nb(Ta)–O3 interaction. This leads to an alternation of short and long M–O lengths in the ··· O–Nb(Ta)–O–Nb(Ta)–O ··· chains that extend along the b axis. The transposition of the Nb–O3 short, long distances amounts to a difference of 0.44 Å, which compares with the smaller difference of 0.10 Å for the corresponding Ta–O3 interactions (cf. Table 3). These distances are consistent with the expected relative magnitudes of the $4d\pi$–$2p\pi$ vs $5d\pi$–$2p\pi$ metal–oxygen interactions that contribute to the Nb(Ta)–O bonding and the observed distortions (13).

These compounds crystallize in the polar point group $mm2$, and, as such, each is expected to have a permanent dipole moment directed along the c axis. The B_2O_5 groups, approximately directed along this axis, should make a major contribution to the net moment. A contribution from the Nb(Ta)-centered octahedra should be associated with displacement of the Nb(Ta) atoms along the c axis within the O1, O2 equatorial plane. The Nb atom is slightly displaced toward the O1 atoms (cf. Table 3), but in the case of

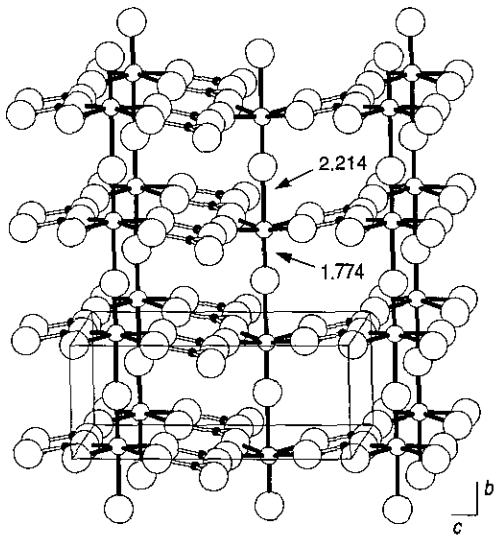

FIG. 2. Drawing of $NbOB_2O_5$ framework in the compound $CsNbOB_2O_5$.

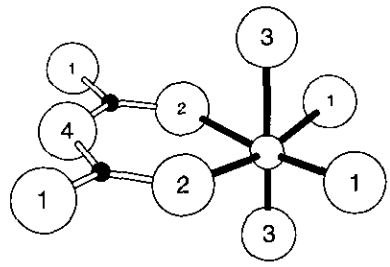

FIG. 3. NbB_2O_9 unit of $CsNbOB_2O_5$.

TABLE 3
Selected Interatomic Distances (Å) and Angles (°) for $CsMOB_2O_5$

	M = Nb	M = Ta		M = Nb	M = Ta
Cs–O1 (×2)	3.313(5)	3.28(2)	O1–Cs–O1	51.2(2)	47.2(7)
Cs–O2 (×2)	3.231(5)	3.17(2)	O2–Cs–O2	78.0(1)	76.8(3)
Cs–O2 (×2)	3.101(5)	3.11(2)		97.1(2)	100.3(6)
Cs–O4	3.160(6)	3.17(2)		164.5(1)	166.7(6)
Cs–O4	3.196(7)	3.21(2)		102.7(2)	100.3(6)
			O2–Cs–O1	84.6(1)	81.7(6)
				42.1(1)	39.5(4)
				102.7(2)	90.4(4)
				122.3(1)	124.7(5)
				81.9(1)	83.2(5)
			O1–Cs–O4	153.87(9)	155.8(4)
				105.9(1)	98.3(4)
			O2–Cs–O4	74.2(1)	73.1(3)
				119.38(9)	118.7(3)
			O4–Cs–O4	77.7(1)	75.5(4)
M–O1(×2)	1.944(4)	1.99(2)	O1–M–O1	94.9(3)	93(1)
M–O2(×2)	2.009(4)	1.98(2)	O1–M–O2	89.2(2)	90.5(7)
M–O3(×1)	2.214(6)	2.009(2)		165.9(2)	170.9(6)
M–O3(×1)	1.774(6)	1.906(2)	O1–M–O3	95.9(2)	96.5(9)
				83.8(2)	88.9(8)
			O2–M–O2	83.8(2)	85.2(9)
			O2–M–O3	83.2(2)	82.7(8)
				97.2(3)	91.5(9)
			O3–M–O3	179.5(5)	172(2)
B–O1	1.343(7)	1.31(3)	O1–B–O2	121.0(6)	120(2)
B–O2	1.362(7)	1.37(2)	O1–B–O4	123.0(6)	118(2)
B–O4	1.394(7)	1.41(2)	O2–B–O4	116.0(5)	121(2)

the Ta analog, Ta–O1 and Ta–O3 distances are statistically equivalent. Another source of a moment from these octahedra would be a deviation of the angle O3–Nb(Ta)–O3 from linearity. As seen in the Table 3, there is no statistically significant distortion.

The presence of the · · · O–Nb–O–Nb–O · · · chain with short and long Nb–O distances is an intriguing structural feature that is reminiscent of a similar chain (· · · O–Ti–O–Ti–O · · ·) in the commonly used nonlinear optical material KTP ($KTiOPO_4$) (14). An individual · · · O–Nb–O–Nb–O · · · chain from the $CsNbOB_2O_5$ structure, or a collection of such chains appropriately aligned, would produce a permanent dipole moment and might be expected to produce a significant optical nonlinearity. But, in the structure of $CsNbOB_2O_5$ these chains are oriented orthogonal to the polar crystal axis. Adjacent chains are then related by the 2_1 screw axis along the c axis, which effectively reverses the moments of the chains related by this symmetry operation. In effect, for each chain in the cell with a repeat Nb–O distance pattern of short, long, short, long, there is the opposite pattern of long, short, long, short. The chains may be considered to be related by a center of symmetry, and they will not contribute to the net dipole moment or significantly to the second-order nonlinear optical susceptibility.

From structural considerations alone, it appears that the orientations of the B_2O_5 groups make the greatest contribution to the dipole moment. These same considerations are applicable when considering the second-order optical susceptibilities of these materials. The nonlinear optical properties should derive from the borate substructure; we note that the magnitudes of the reported nonlinearities are consistent with this assertion.

The structures of the Rb and K analogs, $RbNbOB_2O_5$ and $KNbOB_2O_5$, are similar to the Cs compound, except the Rb compound exhibits a supercell approximately $5 \times b$ and the K compound exhibits a supercell approximately $8 \times b$. A drawing of the structure of the K compound is given in Fig. 4. Because of the smaller size of the K atom, greater deviations from coplanarity are seen in the arrange-

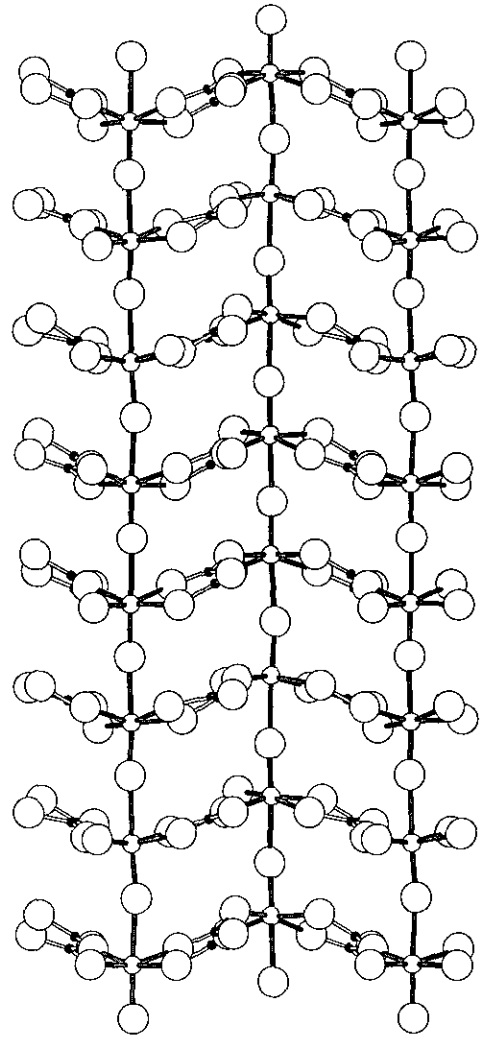

FIG. 4. Drawing of $NbOB_2O_5$ framework in the compound $KNbOB_2O_5$ (cf. Fig. 2).

TABLE 4
Lattice Parameters for Solid Solutions

	$K_{1-x}Rb_xNbOB_2O_5$				$Rb_{1-x}Cs_xNbOB_2O_5$			
x	a (Å)	b (Å)	c (Å)	V (Å)	a (Å)	b (Å)	c (Å)	V (Å^3)
0	7.315(1)	3.904(4)	9.210(4)	263.1(2)	7.389(3)	3.928(5)	9.449(3)	274.2(2)
0.2	7.343(2)	3.866(6)	9.303(7)	264.1(6)	7.468(5)	3.944(9)	9.411(5)	277.2(4)
0.4	7.319(8)	3.814(8)	9.300(1)	265.7(8)	7.472(2)	3.950(2)	9.450(2)	278.8(2)
0.5	7.330(2)	3.912(3)	9.379(3)	268.9(3)	7.469(2)	3.956(3)	9.499(2)	280.6(3)
0.6	7.361(7)	3.914(8)	9.381(7)	270.3(8)	7.465(4)	3.965(6)	9.508(5)	281.5(8)
0.8	7.486(6)	3.907(2)	9.329(5)	272.5(7)	7.555(4)	3.972(7)	9.456(5)	283.7(7)
1	7.389(3)	3.928(2)	9.449(3)	274.2(2)	7.457(2)	3.992(2)	9.710(5)	289.1(2)

ment of the B_2O_5 groups. These deviations gradually decrease, and a more coplanar arrangement of the groups is observed as the size of the alkali-metal atom increases in the series K → Rb → Cs. In this series the average interplanar angle between the B_2O_5 groups decreases from approximately 50° in the K compound to 40° in the Rb derivative and to 4° in the Cs compound. The more highly coplanar arrangement should also produce a larger birefringence—and this has been experimentally verified. The K compound does not possess a sufficient birefringence to phase match 1 − μm light for second-harmonic generation, while the Rb analog does have a sufficient birefringence ($\Delta n_{max} = 0.033$) for phase matching. Again, because of the greater coplanarity among the B_2O_5 groups in the Cs analogs, we expect them to have the highest birefringence.

The magnitude of the birefringence is also expected to vary systematically within the solid–solution series $Rb_{1-x}Cs_xNbOB_2O_5$ and $Rb_{1-x}K_xNbOB_2O_5$ ($0 < x < 1$).

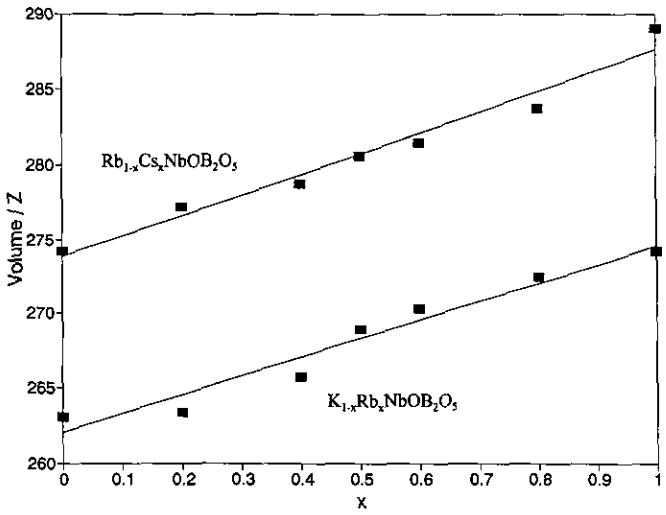

FIG. 5. Plots of unit-cell volume per formula unit vs composition for the solid-solution series $K_{1-x}Rb_xNbOB_2O_5$ and $Rb_{1-x}Cs_xNbOB_2O_5$ ($0 \leq x \leq 1$).

We have studied these series with powder X-ray diffraction techniques; the data are summarized in Table 4, and the results are presented in Fig. 5. In assembling these data, we considered only the subcell reflections, and no attempts were made to identify the potential supercells associated with each composition. Nevertheless, steadily increasing unit-cell volumes per formula unit for substitution of Rb for K and Cs for Rb indicate complete solid solubility across the series (Fig. 5). The intermediate compositions may well exhibit unusual super- or modulated structures, and they should also have intermediate levels of birefringence.

In summary, the crystal chemistry associated with these pyroborates provides an opportunity to produce materials with useful properties for second-harmonic generation. The nonlinearity and birefringence associated with the compounds $CsNbOB_2O_5$ and $CsTaOB_2O_5$ make them promising candidates for frequency doubling 1 − μm laser light. Their use as bulk single crystals, however, may be limited by their mechanical durability.

ACKNOWLEDGMENT

This work was supported by the U.S. National Science Foundation, Solid-State Chemistry Program (DMR-9221372).

REFERENCES

1. M. Gasperin, *Acta Crystallogr., Sect. B* **30,** 1182 (1974).
2. B. Cerville, F. Cesbron, J. Berth, and P. Jollies, *Acta Crystallogr., Sect. A* **30,** 645 (1974).
3. A. Baucher and M. Gasperin, *Mater. Res. Bull.* **10,** 469 (1974).
4. A. Baucher and M. Gasperin, *Acta Crystallogr., Sect. B* **32,** 2211 (1976).
5. J. F. H. Nicolls, B. H. T. Chai, D. L. Corker, J. C. Calabrese, and B. Henderson, *Proc. SPIE-Int. Soc. Opt. Eng.* **1863,** 54 (1993).
6. G. Loiacono, Crystal Associates, Inc., private communication.
7. TEXSAN: Single Crystal Structure Analysis Software, Version 5.0, Molecular Structure Corporation, The Woodlands, TX, 1989.
8. G. M. Sheldrick, *in "Crystallographic Computing 3"* (G. M. Sheldrick, C. Krüger, and R. Goddard, Eds.), p. 175. Oxford Univ. Press, London, 1985.

9. N. Walker and D. Stuart, *Acta Crystallogr., Sect. A* **39,** 158 (1983).
10. D. T. Cromer and J. T. Waber, *in* "International Tables for X-ray Crystallography," Vol. IV, Table 2.2A. Kynoch Press, Birmingham, UK, 1974.
11. R. D. Shannon, *Acta Crystallogr., Sect. A* **32,** 751 (1976).
12. P. D. Thompson, J. Huang, R. W. Smith, and D. A. Keszler, *J. Solid State Chem.* **95,** 126 (1991).
13. R. A. Wheeler, M-H. Whangbo, T. Hughbanks, R. Hoffmann, J. K. Burdett, and T. A. Albright, *J. Am. Chem. Soc.* **107,** 2222 (1986).
14. J. D. Bierlein and H. Vanherzeele, *J. Opt. Soc. Am. B: Opt. Phys.* **6,** 622 (1989).